

## An updated 1-dimensional seismic velocity model has been developed for the $M_w$ 6.1 Pasaman earthquake that occurred on February 25, 2022

Bertalina Sihotang<sup>1,2</sup>, Syahrul Humaidi<sup>1\*</sup>, Andrean V. H. Simanjuntak<sup>2</sup>

<sup>1</sup> Post Graduate Program (Physics), FMIPA, Universitas Sumatera Utara, Medan, Sumatra Utara, Indonesia

<sup>2</sup> Agency of Meteorological Climatology and Geophysical for Indonesia, Medan, Sumatra Utara, Indonesia

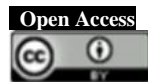
\*Corresponding author e-mail: [syahrull@usu.ac.id](mailto:syahrull@usu.ac.id)

Received: March, 23 2024

Accepted: June 05, 2024

Published: June 05, 2024

Copyright © 2024 by author(s) and Scientific Research Publishing Inc.



### Abstract

On February 25, 2022, a strong-felt earthquake with magnitude  $M_w$  6.1 occurred within the western portion of Pasaman, West Sumatra, Indonesia. The impact of the seismic activities has produced an enormous shaking which measured as VI on the Adjusted Mercalli Concentrated (MMI) and II -III MMI until Malaysian and Singapore region. The casualty's reports contain the data approximately the broadly harms such as, 1765 residences and murdered at slightest 18 individuals in West Sumatra Area. A dependable dynamic blame was already unidentified and raise a major address almost the association with Sumatra dynamic blame. Therefore, this analysis examines the attributes of seismic activity and the damage caused by utilizing an appropriate 1-Dimensional seismic velocity model. The acquired 1-Dimensional speed data exhibits varying values at a depth of 10 km with a velocity of approximately 5.5 km/s and at 30 km with a velocity of approximately 7 km/s. The 1-D velocity obtained exhibits a parallel and distinctive pattern with an RMS value of less than 1.0. In addition, the PGA records reveal a seismic intensity of 10% in Pasaman, consistent with the damage reports obtained during field assessments. This indicates that Pasaman is located in a zone with frequent seismic activity.

**Keywords:** Earthquake, Seismic, Peak Ground Acceleration (PGA), Peak Ground Velocity (PGV), Seismic Velocity, Hypocenter

### 1. Introduction

A seismic event with a magnitude of 6.1 on the Moment Magnitude Scale ( $M_w$ ) took place in the western region of Pasaman, located in West Sumatra, Indonesia, on February 25, 2022. The exact location of the earthquake is indicated by a yellow star in Figure 1. The mainshock was preceded by a foreshock with a magnitude of 5.1 on the moment magnitude scale ( $M_w$ ). Indonesian Agency for Meteorological, Climatological, and Geophysical Agency (BMKG) reported that the effect of the earthquake has provided a widely ground shaking which measured as VI on the Modified Mercalli Intensity (MMI) and II -III MMI until Malaysian and Singapore ([www.bmkg.go.id/](http://www.bmkg.go.id/)). The casualty's reports contain the information about the widely damages such as, 1765 dwellings and killed at least 18 people in West Sumatra Province ([www.bnpb.go.id/](http://www.bnpb.go.id/)). A responsible active fault was previously unidentified and raise a major question about the connection with Sumatra active fault.

The earthquake took place at a shallow depth of 10 km and indicates the presence of an active fault in the Earth's crust. The fault mechanism solution

provided by geophysical institutions such as the United States Geological Survey (USGS), the Global Centroid Moment Tensor (GCMT), GFZ, and IGP indicates that the rupture takes place along the fault, moving in a rightward direction in the Northeast - Southwest (NE - SW) orientation. The Pasaman area is situated in close proximity to the active fault of the Sumatra fault segmentation. This fault has a slip rate of 1-2cm/year in the right-lateral direction, which might potentially result in significant shaking (Sieh and Natawidjaja, 2000, McCaffrey, 2009). Historically, this area has experienced several major earthquakes with  $M_w > 6.0$  such as  $M_w$  6.1 (March 8, 1977) Sumatran fault event, the  $M_w$  6.4 (March 6, 2007) as the doublet earthquake phenomena, and  $M_w$  7.6 (September 30, 2009) as the intra-slab earthquake, the references cited are Bradley et al. (2017), Pasari et al. (2021), and Nurana et al. (2022).

A few studies about have been published recently such as, Pasari et al., (2021) examined the risk level utilizing nowcasting examination within the Sumatra region and most current considers from Supendi et al. (2022) that conducted a comprehensive investigation

around Pasaman seismic tremor utilizing hypocenter migration, finite-fault inversion and moment tensor inversion. Be that as it may, Supendi et al., (2022) did not give the upgraded 1-D speed show as the input for hypocenter movement. Subsequently, we attempt to consider the seismic tremor dissemination by collecting the entry time of the seismic stage (P and S). Besides, there's less ponder that has been carried out on the 2022 Pasaman seismic tremor and its results for seismic potential dangers.

As a result, this ponder explores the location of the seismic tremor hypocenter by calculating the correct

speed demonstrate, permitting for an progressed position of the hypocenter. The exactness of the seismic tremor characteristics is fundamental for future seismic tremor moderation methodologies and recognizing potential seismic dangers in this locale. Determining the location of an earthquake involves several factors that affect the accuracy of the results, including determining the arrival time of seismic waves and using one-dimensional wave speed models that are appropriate for the geographical and geological conditions.

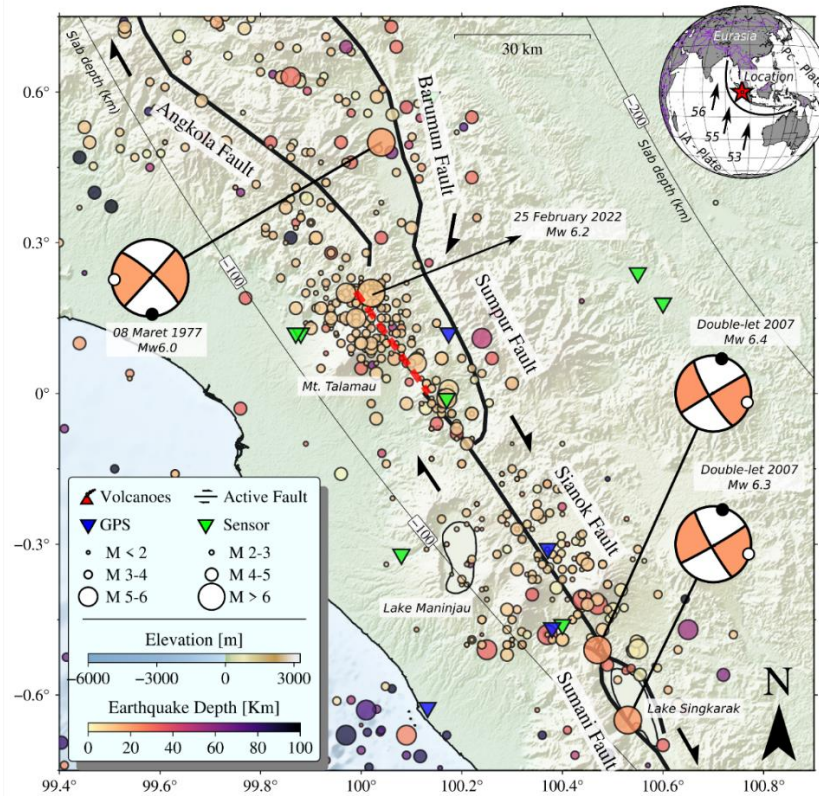


**Figure 1.** displays a seismotectonic map of the West Sumatra Province, highlighting the Pasaman 2022 Mw 6.1 earthquake with a black arrow. The historical focusing mechanisms were obtained from the GCMT catalogue. The active Sumatran fault is represented by the black line, the seismic site is indicated by the green triangle, and the GPS site is denoted by the blue triangle.

## 2. Methods

### 2.1 Geiger Method

The determination of the earthquake site is a pivotal subject in seismology since it can offer a comprehensive understanding of the source mechanism's intricate structure. The Geiger method, which utilizes a linearization approach, is often employed for processing of earthquakes. The hypocenter parameters  $(x_0, y_0, z_0, t_0)$  and origin time of observation are compared with the calculation model to determine the residual trip time. The Taylor series, as shown in equation (1), can be used to compute the errors  $(\Delta x, \Delta y, \Delta z, \text{ dan } \Delta t)$  that need to be minimized.

$$r = \frac{\partial t_i^{tra}}{\partial x_i} \Delta x + \frac{\partial t_i^{tra}}{\partial y_i} \Delta y + \frac{\partial t_i^{tra}}{\partial z_i} \Delta z + \Delta t \quad (1)$$

Equation (1) can be expressed in the form of an inversion, denoted as equation (2), and represented in matrix form, denoted as equation (3).

$$\mathbf{d} = \mathbf{Gm} \quad (2)$$

$$\begin{bmatrix} d_1 \\ \dots \\ d_n \end{bmatrix} = \begin{bmatrix} \frac{\partial t_i^{tra}}{\partial x_0} & \frac{\partial t_i^{tra}}{\partial y_0} & \frac{\partial t_i^{tra}}{\partial z_0} & 1 \\ \dots & \dots & \dots & \dots \\ \frac{\partial t_i^{tra}}{\partial x_n} & \frac{\partial t_i^{tra}}{\partial y_n} & \frac{\partial t_i^{tra}}{\partial z_n} & 1 \end{bmatrix} \begin{bmatrix} \Delta x \\ \Delta y \\ \Delta z \\ \Delta t \end{bmatrix} \quad (3)$$

R can be classified as the residual vector, G is the partial derivative matrix, and x represents the adjustment vector for earthquake location and origin time. The hypocenter and origin time will be simultaneously rectified by adding  $\Delta x, \Delta y, \Delta z,$  and  $\Delta t$  to their respective coordinates. Subsequently, the solution is employed in the subsequent iteration phase. The iteration procedure persists until reaching a preset threshold or yielding a minimal residual (Havskov and Ottemöller, 1999).

## 2.2 Coupled Hypocenter-Velocity

We utilized a coupled-hypocenter method that has the capability to concurrently determine an updated hypocenter location, revise the local 1-D seismic velocity model, and rectify the quality of the seismic station (Kissling, 2002). The underlying procedure of the coupled-hypocenter method involves a non-linear inversion using a linear methodology, as seen in equation (4). Equation (4) defines the variables used in seismic analysis. The variable  $t_{obs}$  represents the arrival time of the earthquake at each earthquake sensor. The variable  $s$  represents the origin time of the earthquake. The variable  $h$  represents the calculated hypocenter position. The variable  $m$  represents the velocity model utilized.

$$t_{obs} = f(s, h, m) \quad (4)$$

$f$  is a function that is not linear and depends on parameters that are currently unknown. By utilizing the beginning velocity model and applying the wave propagation theory, the equation (5) may be used to express the theoretical wave arrival time  $t_{cal}$  for each pair of stations,

$$t_{cal} = f(h_j, m_k) \quad (5)$$

$h_j$  is the theoretical origin time and  $m_k$  is the velocity model given. In other hand,  $t_{cal}$  needs to be compared with  $t_{obs}$  as the  $t_{res} = t_{obs} - t_{cal}$  to derive the residual time  $t_{res}$  as shown in the proof (6):

$h_j$  represents the theoretical starting time, while  $m_k$  represents the provided velocity model. On the other hand, it is necessary to compare  $t_{cal}$  with  $t_{obs}$  in order

to calculate the residual time  $t_{res}$ , which is given by the equation  $t_{res} = t_{obs} - t_{cal}$ , as demonstrated in proof (6).

$$t_{res} = \sum_{j=1}^4 \frac{\partial f}{\partial h_j} \Delta h_j + \sum_{k=1}^n \frac{\partial f}{\partial m_k} \Delta m_k + e \quad (6)$$

- $j$  = total earthquakes;
- $k$  = total seismic stations;
- $\Delta m_k$  = parameter model;
- $\Delta h_j$  = parameter hypocenter;

In equation (6),  $e$  represents the error used to calculate the station correction. Several research studies have employed Velest to determine a 1-Dimensional seismic velocity model. For example, Simanjuntak et al. (2022) conducted migration studies in the Southeast Aceh region, while Muksin et al. (2023) investigated local structural features in the East Aceh region.

## 3. Results and Discussion

### 3.1 1-D Seismic Velocity Model

The availability of high-precision seismic velocity models at local-regional scales is a crucial factor in determining the accuracy of seismic hypocenter location. Encourage investigation is required to get it the characteristics of the causal flaws. Hypocenter relocations are connected to more precisely resolve hypocenter precise location based on suitable and updated seismic 1-D velocity models.

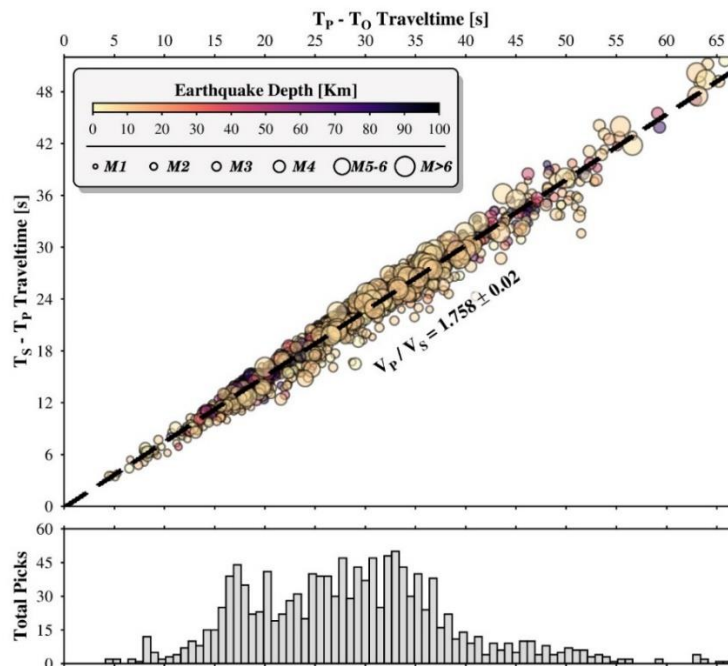


**Figure 2.** The correlation between the traveltime of S-P waves and the arrival time of the P and S phases is influenced by factors such as the root mean square (RMS), depth, number of seismic events and phases, and the value of the  $V_p/V_s$  ratio, which is around 1.76. The difference in duration between the P and S stages is 40 seconds, whereas the time it takes for the P and S stages to begin is -96 seconds. The precision of determining the P and S phases is -5 and 5 seconds.

This early study involved analyzing 170 seismic tremor events ranging from magnitudes M 2.0 to 5.8. For all the events examined, a total of 1011 P-phases and 641 S-phases were recorded by 24 stations. The ratio of  $V_p$  (compressional wave velocity) to  $V_s$  (shear wave velocity) was approximately 1.73, as shown in Figure 2. The hypocenters in the BMKG catalog are located at depths of 10 and 33 km. In order to improve the accuracy of the hypocenter area, it is crucial to find suitable one-dimensional models. In this analysis, a set of 100 pre-existing models, as shown in Figure 3, were used to obtain focused results (RMS < 1.0) by simultaneous execution of 50 iterations.

The focalized demonstrate is the most suitable method for determining the initial and final movement of the hypocenter and for determining the characteristics of the earthquake source (Qadaryah et al., 2018, Simanjuntak and Ansari, 2022). In Figure 3, the results of the study were selected since it contains a larger amount of data and represents the entire Pasaman region. The obtained speed models include the velocities of body waves, specifically P waves and S waves, as well as the ratio between P and S waves. The root mean square (RMS) value of each demonstration will decrease with each cycle, as it is calculated using a least-square synchronous reversal process.

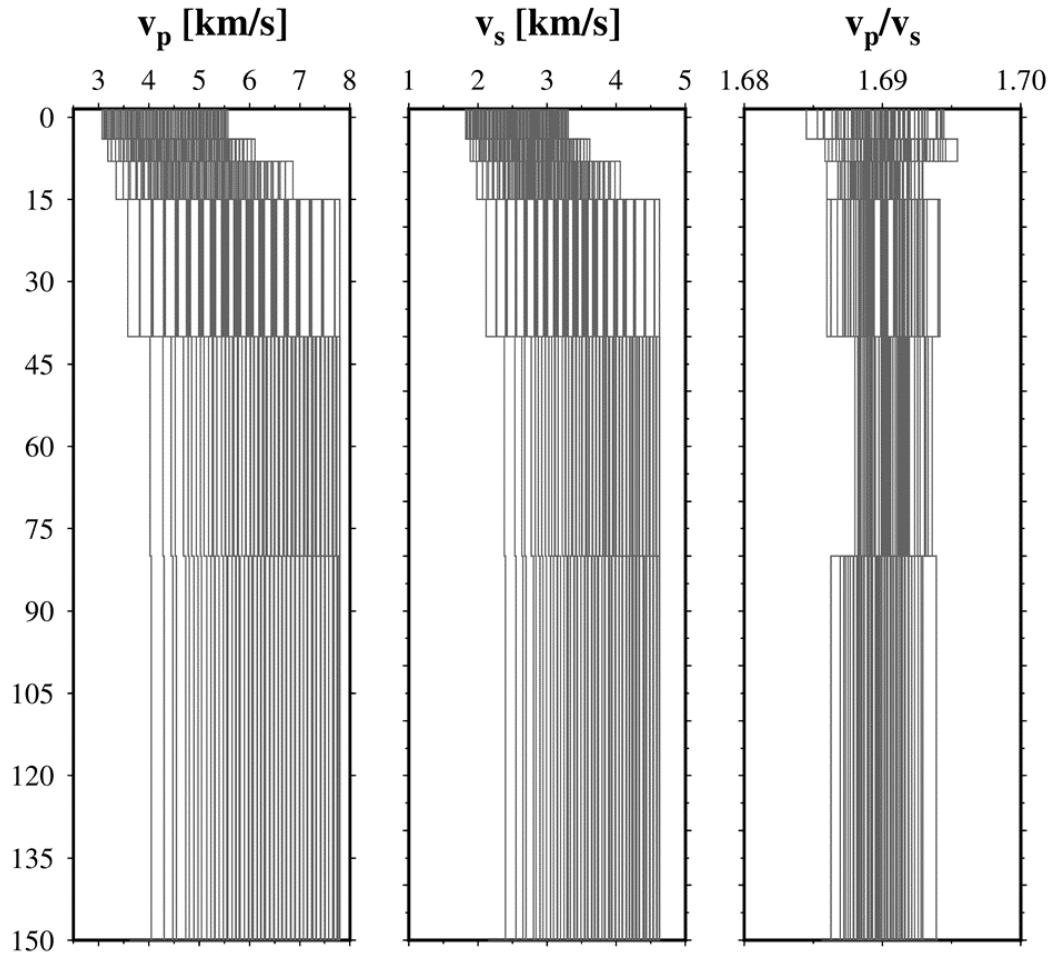


Figure 3. 100 initial velocity models were used for the inversion process.

The RMS esteem is unique due to the availability of a priori data, which can have both low and high values. The optimal RMS value is generally less than 1.0 s. The RMS value of less than 1.0 s is highly desirable for transit between territorial stations, as these stations are located far apart.

Table 1. Final 1-D velocity model in the Pasaman region with depth ranging 0 – 100km.

Depth (km)	Vp (km/s)	Vs (km/s)
0.00	4.02	2.88
4.00	4.43	2.95
8.00	5.40	3.12

12.00	5.49	3.41
20.00	5.86	3.56
30.00	5.86	3.90
40.00	8.03	4.58
60.00	8.71	4.72
80.00	8.75	4.75
100.00	8.75	4.75

As the material transitions from a more fluid state to a solid state and the location of the hypocenter becomes clearer, as depicted in Figure 4, the seismic wave velocity will increase and exhibit a direct

relationship with the depth. In order to create an appropriate 1-dimensional model, it is necessary to select hypocenters that meet the predetermined parameter constraints set during the inversion process. In this investigation, the optimal model was determined by selecting an RMS < 1.0 s, an RMS  $\geq$  1.0 for 11 earthquakes, and an RMS = 0.9 s for the 1-D model. Comparing the model with pre-relocation data to the data without relocation data, the former has more hypocenters with better rms.

The increased sample size and inclusion of nearly all locations contribute to the greater consistency of these results in terms of variances. Furthermore, a notable link has been seen between  $T_p$  and  $T_s$ , and the impact on  $V_p/V_s$  is around 1.73. The  $V_p/V_s$  values after relocation exhibit the lowest number of misfit values, the strongest correlations with minimal deviations, and a limited distribution of outliers in  $T_p$  and  $T_s$ .

The ground motion measurement indicates that the PGA (Peak Ground Acceleration) and PGV (Peak Ground Velocity) models, with a PGA value ranging from 0 to 15% gal and a PGV value ranging from 0 to 8 cm/s<sup>2</sup>, accurately correspond to the intensity of the earthquake experienced by the local population in Pasaman. Furthermore, a recommended threshold for MMI ~6 is a maximum acceleration of approximately 110 cm/s<sup>2</sup>, which corresponds to a 10% gal. This limit is considered reasonable for determining serious and accountable harm.

Atkinson (2020) conducted a study comparing artificial and natural earthquakes and discovered that seismic ground acceleration (PGA) with a frequency higher than 5 Hz can occur, while seismic ground velocity (PGV) between the 0.5-7 Hz range can lead to structure damage. PGV is generally linked to strong earthquake intensities, whereas PGA is frequently related to the impact experienced at weak earthquake intensities.

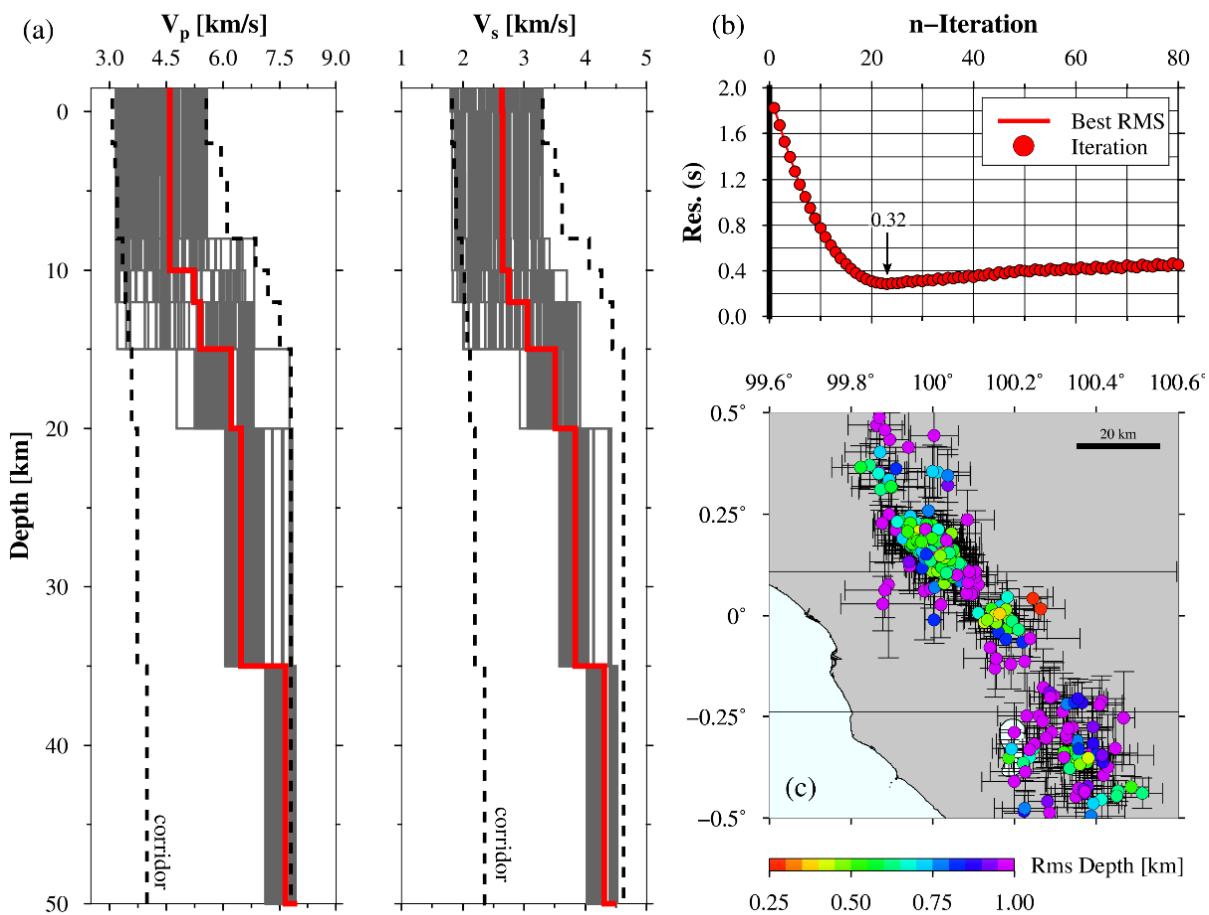


**Figure 4.** The final velocity model (a) shown by the red line was determined by simultaneous inversion. The left panel displays the P-wave velocity, while the center panel displays the S-wave velocity. (b) The graph displaying the root mean square (rms) outcome following simultaneous inversion. The hypocenter was relocated using an improved 1-D velocity model that accurately corresponds to the fault line responsible for the seismic activity in the study area (c).

Therefore, PGA (Peak Ground Acceleration) and PGV (Peak Ground Velocity) are widely acknowledged as the most valuable metrics for assessing the excellence of building. Moreover, it is imperative to conduct a thorough and extensive investigation to fully understand the seismotectonics of the Pasaman earthquake and mitigate the potential risks in the coming years.

## 5. Conclusions

The findings of the investigation allow us to draw the following conclusions. The one-dimensional nearby velocity display consists of multiple layers. The velocity of the object is around 5.5 kilometers per second at a depth of 10 kilometers. The velocity of the object is around 7 kilometers per second, and it is located at a depth of 30 kilometers. The 1-D

seismic velocity model obtained using simultaneous inversion exhibits a focused and intriguing layout, with an RMS value of less than 1.0. Pasaman exhibits the most prominent PGA (Peak Ground Acceleration) and PGV (Peak Ground Velocity) values, as determined by the ground motion analysis conducted post-migration. The PGA data reveal a seismic hazard rate exceeding 10% in Pasaman, consistent with the damage reports obtained during field assessments. This indicates that Pasaman is located in a region with frequent seismic activity. Additional research might be undertaken specifically to investigate disaster mitigation in the Pasaman region.

## Acknowledgements

We express our gratitude to the Badan Meteorologi Klimatologi dan Geofisika (BMKG) for their provision of the seismic data. We express our gratitude to our colleagues at the BMKG office in the 1st regional in Medan for engaging in a productive discussion regarding the tectonic system in the Pasaman area.

## References

- Adi, S. P., Simanjuntak, A. V., Supendi, P., Wei, S., Muksin, U., Daryono, D., ... & Sinambela, M. (2024). Different Faulting of the 2023 (Mw 5.7 and 5.9) South-Central Java Earthquakes in the Backthrust Fault System. *Geotechnical and Geological Engineering*, 1-13.
- Asnawi, Y., Simanjuntak, A. V. H., Muksin, U., Okubo, M., Putri, S. I., Rizal, S., & Syukri, M. (2022). Soil classification in a seismically active environment based on joint analysis of seismic parameters. *Global Journal of Environmental Science and Management*, 8(3), 297-314.
- Asnawi, Y., Simanjuntak, A., Muksin, U., Rizal, S., Syukri, M. S. M., Maisura, M., & Rahmati, R. (2022). Analysis of Microtremor H/V Spectral Ratio and Public Perception for Disaster Mitigation. *GEOMATE Journal*, 23(97), 123-130.
- Atkinson, G. M. (2020). The Intensity of Ground Motions from Induced Earthquakes with Implications for Damage Potential. *The Intensity of Ground Motions from Induced Earthquakes with Implications for Damage Potential. Bulletin of the Seismological Society of America*, 110(5), 2366-2379.
- Bradley, K. E., Feng, L., Hill, E. M., Natawidjaja, D. H., & Sieh, K. (2017). Implications of the diffuse deformation of the Indian Ocean lithosphere for slip partitioning of oblique plate convergence in Sumatra. *Journal of Geophysical Research: Solid Earth*, 122(1), 572-591.
- Havskov, J., & Ottemoller, L. (1999). SEISAN earthquake analysis software. *Seismol. Res. Lett*, 70(5), 532-534.
- Idha, R., Sari, E. P., Asnawi, Y., Simanjuntak, A. V., Humaidi, S., & Muksin, U. (2023). 1-Dimensional Model of Seismic Velocity after Tarutung Earthquake 1 October 2022 Mw 5.8. *Journal of Applied Geospatial Information*, 7(1), 825-831.
- Idha, R., Sari, E. P., Humaidi, S., Simanjuntak, A. V., & Muksin, U. (2023, December). Response of Geologic Units to The Ground Parameters of Tarutung Earthquake 2022 Mw 5.8: A Preliminary Study. In *IOP Conference Series: Earth and Environmental Science* (Vol. 1288, No. 1, p. 012032). IOP Publishing.
- Idha, R., Sari, E. P., Humaidi, S., Simanjuntak, A. V., & Muksin, U. (2023). Model Kecepatan Seismik 1-Dimensi Pada Wilayah Gempa Bumi Tarutung 2022 Mw 5.8. *Kesatria: Jurnal Penerapan Sistem Informasi (Komputer dan Manajemen)*, 4(2), 469-477.
- Irwandi, I., Muksin, U., & Simanjuntak, A. V. (2021). Probabilistic seismic hazard map analysis for Aceh Tenggara district and microzonation for Kutacane city. In *IOP Conference Series: Earth and Environmental Science* (Vol. 630, No. 1, p. 012001). IOP Publishing.
- Kissling, E., U. Kradolfer, and H. Maurer. "Program VELEST user's guide-Short Introduction." Institute of Geophysics, ETH Zurich (1995).
- McCaffrey, R. (2009). The tectonic framework of the Sumatran subduction zone. *Annual Review of Earth and Planetary Sciences*, 37, 345-366.
- Muksin, U., Arifullah, A., Simanjuntak, A. V., Asra, N., Muzli, M., Wei, S., ... & Okubo, M. (2023). Secondary fault system in Northern Sumatra, evidenced by recent seismicity and geomorphic structure. *Journal of Asian Earth Sciences*, 105557.
- Nurana, I., Simanjuntak, A. V. H., Umar, M., Kuncoro, D. C., Syamsidik, S., & Asnawi, Y. (2021). Spatial Temporal Condition of Recent Seismicity In The Northern Part of Sumatra. *Elkawanie: Journal of Islamic Science and Technology*, 7(1), 131-145.
- Pasari, S., Simanjuntak, A. V., Mehta, A., Neha, & Sharma, Y. (2021). A synoptic view of the natural time distribution and contemporary earthquake hazards in Sumatra, Indonesia. *Natural Hazards*, 108, 309-321.
- Pasari, S., Simanjuntak, A. V., Mehta, A., Neha, & Sharma, Y. (2021). The current state of earthquake potential on Java Island, Indonesia. *Pure and Applied Geophysics*, 178, 2789-2806.
- Pasari, S., Simanjuntak, A. V., Neha, & Sharma, Y. (2021). Nowcasting earthquakes in Sulawesi island, Indonesia. *Geoscience Letters*, 8, 1-13.
- Qadariah, Q., Simanjuntak, A. V., & Umar, M. (2018). Analysis of Focal Mechanisms Using Waveform Inversion; Case Study of Pidie Jaya Earthquake December 7, 2016. *Journal of Aceh Physics Society*, 7(3), 127-132.

- Sari, E. P., Idha, R., Asnawi, Y., Simanjuntak, A., Humaidi, S., & Muksin, U. (2023). Faulting Mechanism of Tarutung Earthquake 2022 Mw 5.8 Using Moment Tensor Inversion. *Journal of Applied Geospatial Information*, 7(1), 840-846.
- Sari, E. P., Idha, R., Nugroho, H., Humaidi, S., Simanjuntak, A. V., & Muksin, U. (2023). Model Mekanisme Patahan Gempa Bumi Tarutung 2022 Mw 5.8. *Kesatria: Jurnal Penerapan Sistem Informasi (Komputer dan Manajemen)*, 4(2), 478-486.
- Sieh, K., & Natawidjaja, D. (2000). Neotectonics of the Sumatran fault, Indonesia. *Journal of Geophysical Research: Solid Earth*, 105(B12), 28295-28326.
- Simanjuntak, A. V., & Ansari, K. (2022). Seismicity clustering of sequence phenomena in the active tectonic system of backthrust Lombok preceding the sequence 2018 earthquakes. *Arabian Journal of Geosciences*, 15(23), 1730.
- Simanjuntak, A. V., & Ansari, K. (2024). Multivariate Hypocenter Clustering and Source Mechanism of 2017 Mw 6.2 and 2019 Mw 6.5 in the South Seram Subduction System. *Geotechnical and Geological Engineering*, 1-14.
- Simanjuntak, A. V., Kuncoro, D. C., Irwandi, I., & Muksin, U. (2022). Understanding swarm earthquakes in Southeast Aceh, Sumatra. In *E3S Web of Conferences* (Vol. 339, p. 02011). EDP Sciences.
- Simanjuntak, A., Muksin, U., Asnawi, Y., Rizal, S., & Wei, S. (2022). Recent Seismicity and Slab Gap Beneath Toba Caldera (Sumatra) Revealed Using Hypocenter Relocation Methodology. *Geomate Journal*, 23(99), 82-89.
- Supendi, P., Rawlinson, N., Prayitno, B. S., Sianipar, D., Simanjuntak, A., Widiyantoro, S., ... & Sudrajat, A. (2023). A previously unidentified fault revealed by the February 25, 2022 (Mw 6.1) Pasaman earthquake, West Sumatra, Indonesia. *Physics of the Earth and Planetary Interiors*, 334, 106973.
- Worden, C. B., Gerstenberger, M. C., Rhoades, D. A., & Wald, D. J. (2012). Probabilistic relationships between ground-motion parameters and modified Mercalli intensity in California. *Bulletin of the Seismological Society of America*, 102(1), 204-221.